

# Taste More, Taste Better: Diverse Data and Strong Model Boost Semi-Supervised Crowd Counting

Maochen Yang<sup>1</sup> Zekun Li<sup>1</sup> Jian Zhang<sup>1</sup> Lei Qi<sup>3</sup> Yinghuan Shi<sup>1,2,\*</sup>

<sup>1</sup>Nanjing University, China <sup>2</sup>Suzhou Laboratory, China <sup>3</sup>Southeast University, China

{yangmaochen, lizekun, zhangjian7369}@smail.nju.edu.cn qilei@seu.edu.cn, syh@nju.edu.cn

## Abstract

Semi-supervised crowd counting is crucial for addressing the high annotation costs of densely populated scenes. Although several methods based on pseudo-labeling have been proposed, it remains challenging to effectively and accurately utilize unlabeled data. In this paper, we propose a novel framework called Taste More Taste Better (TMTB), which emphasizes both data and model aspects. Firstly, we explore a data augmentation technique well-suited for the crowd counting task. By inpainting the background regions, this technique can effectively enhance data diversity while preserving the fidelity of the entire scenes. Secondly, we introduce the Visual State Space Model as backbone to capture the global context information from crowd scenes, which is crucial for extremely crowded, low-light, and adverse weather scenarios. In addition to the traditional regression head for exact prediction, we employ an Anti-Noise classification head to provide less exact but more accurate supervision, since the regression head is sensitive to noise in manual annotations. We conduct extensive experiments on four benchmark datasets and show that our method outperforms state-of-the-art methods by a large margin. Code is publicly available on [https://github.com/syhien/taste\\_more\\_taste\\_better](https://github.com/syhien/taste_more_taste_better).

## 1. Introduction

Crowd counting is a fundamental task in computer vision that involves estimating the number of people in densely populated scenes. This task is of great importance in various public safety scenarios, including transport manage-

\* Corresponding author: Yinghuan Shi. This work was supported by National Science and Technology Major Project (2023ZD0120700), NSFC Project (62222604, 62206052, 624B2063), China Postdoctoral Science Foundation (2024M750424), Fundamental Research Funds for the Central Universities (020214380120, 020214380128), State Key Laboratory Fund (ZZKT2024A14), Postdoctoral Fellowship Program of CPSF (GZC20240252), Jiangsu Funding Program for Excellent Postdoctoral Talent (2024ZB242), and Jiangsu Science and Technology Major Project (BG2024031).

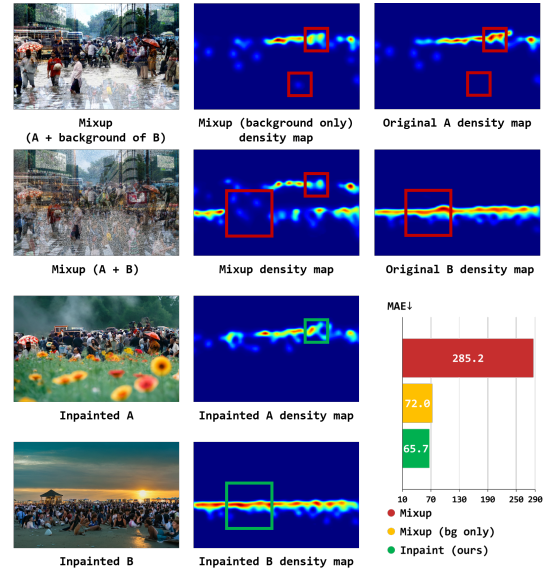


Figure 1. Comparisons of augmentations. As shown in the red bounding boxes, both types of Mixup generate disappointing density maps. Mixup is supposed to retain crowd information from two images, but actually it destroys the spatial structure. As shown in green bounding boxes, our inpainting augmentation is better suited for the crowd counting task, showing an impressive reduction in Mean Absolute Error (MAE).

ment [14, 49, 60] and disaster prevention [50]. The substantial demand has driven the advancement of counting methods [3, 25, 42, 44, 64]. However, a significant cost of manual annotation is unavoidable for these fully-supervised deep methods to achieve satisfactory performance. For example, the UCF-QNRF dataset with 1,535 images and 1,251,642 annotations amounts to approximately 2,000 human-hours [17]. Compared to the extremely expensive labeled data with annotations, acquiring unlabeled crowd images is much more affordable. Consequently, there is a growing interest in leveraging unlabeled data through semi-supervised crowd counting (SSCC) methods. The recent mainstream works on SSCC [21, 24, 39, 67] mostly employ the Mean Teacher [51] framework, where the teacher

model generates pseudo-labels for unlabeled data to guide the student model. The key to achieving superior performance with SSCC methods on a given set of images, where only a small portion is annotated, lies in how we handle the unlabeled samples and how we design an appropriate model to fully exploit the information within them.

It has been observed that introducing similar but different samples to the training data can enlarge the support of the training distribution and thus enhance the robustness and generalizability of the model [4, 45]. In the literature, numerous data augmentation techniques have demonstrated their effectiveness in generating additional virtual samples to support the training process in both fully-supervised and semi-supervised settings [2, 62, 65]. However, we find that these off-the-shelf techniques cannot suit the crowd counting task, as they may destroy the spatial structure of crowd scenes, leading to distorted density maps, as shown in Figure 1. Therefore, a well-suited data augmentation technique specifically designed for the crowd counting task is crucial for the model to *taste more* from the unlabeled data.

With the help of appropriate data augmentation, the diversity of unlabeled data during training can be significantly improved. However, this simultaneously brings new challenges for the teacher model to produce correct supervision signals. From the perspective of the model itself, we find that the Convolutional Neural Network (CNN) architecture commonly used in previous studies can be suboptimal for the crowd counting task, as it tends to overfit to local details and fails to capture global context information, which is crucial for extremely crowded, low-light, and adverse weather scenarios. From another perspective, it is also important to generate more accurate pseudo-labels while filtering out low-quality parts. Considering these two points, we explore a modern backbone network to replace CNNs and enhance it with a holistic strategy for producing and leveraging pseudo-labels, which helps to *taste data better*.

In this paper, we propose a novel semi-supervised crowd counting method, named *Taste More Taste Better* (TMTB). We design a novel data augmentation technique, Inpainting Augmentation, which enhances the diversity of the dataset while keeping the integrity of the foreground regions. Observing that some regions in inpainted images are noisy and harmful, to better utilize the inpainted images, we employ a Visual State Space Model (VSSM) with an Anti-Noise classification branch for assistance, which provides inexact but accurate supervision. The proposed model generates more accurate density maps than state-of-the-art methods. Our method TMTB achieves significant improvements on several benchmark datasets, including ShanghaiTech Part A & B [68], UCF-QNRF [17], and JHU-Crowd++ [46]. We reduce the Mean Absolute Error of JHU-Crowd with 5% data labeled to 67.0, marking the first time it has been lower than 70.0. The method also presents strong generalization ability

in cross-dataset evaluations.

The main contributions of this paper are as follows:

- We observed that the lack of suitable data augmentation methods and the weakness of capturing global context information are bottlenecks for the crowd counting task. The off-the-shelf data methods may destroy the spatial structure of crowd scenes, which is crucial for the regression of density maps. CNNs tend to overfit local details and struggle to capture global context information.
- We propose a novel semi-supervised crowd counting method. A data augmentation technique is designed to enhance diversity while keeping the integrity of the foreground regions. A VSSM with an Anti-Noise classification branch for assistance is employed, which provides inexact but accurate supervision, to better utilize the data.
- The proposed method remarkably outperforms state-of-the-art methods across four benchmark datasets and three label settings. It achieves a groundbreaking reduction in the Mean Absolute Error on the JHU-Crowd dataset with only 5% of the data labeled, lowering it to 67.0, a decrease of 12.4%. Furthermore, the method demonstrates exceptional generalization capabilities in cross-dataset Domain Generalization settings, even surpassing the performance of fully-supervised approaches, setting a new standard for excellence.

## 2. Related Works

**Semi-supervised Crowd Counting.** Fully-supervised crowd counting methods [5, 13, 17, 31, 37, 41, 48, 68] maintain the best performance in crowd counting tasks. However, fully-supervised methods require a large quantity of labeled data, which is expensive to collect and annotate.

Therefore, semi-supervised crowd counting methods have been proposed to address the scarcity of labeled data. The Mean Teacher [51], a successful semi-supervised learning framework that has been widely used in classification [10, 47, 63], segmentation [2, 55] and regression [8, 19, 61], is the most popular method in semi-supervised crowd counting. L2R [26] leveraged unlabeled data through a learning-to-rank framework. IRAST [27] introduced surrogate tasks, self-learning inter-related binary segmentation tasks, to improve performance. Moreover, MTCP [72] applied multiple auxiliary tasks into representation learning, which also benefit performance. DA-Count [23] employed a Transformer [52] to refine foreground features. CU [21] investigated a supervised uncertainty estimation strategy to better utilize unlabeled data. SALCrowd [67] proposed a method to select unlabeled data based on intra-scale uncertainty and inter-scale inconsistency metrics. MRC-Count [39] incorporated a fine-grained density classification task, proving the effectiveness of the classification task in crowd counting. Most previous approaches [21, 26, 27, 39, 67] are based on CNNs or par-

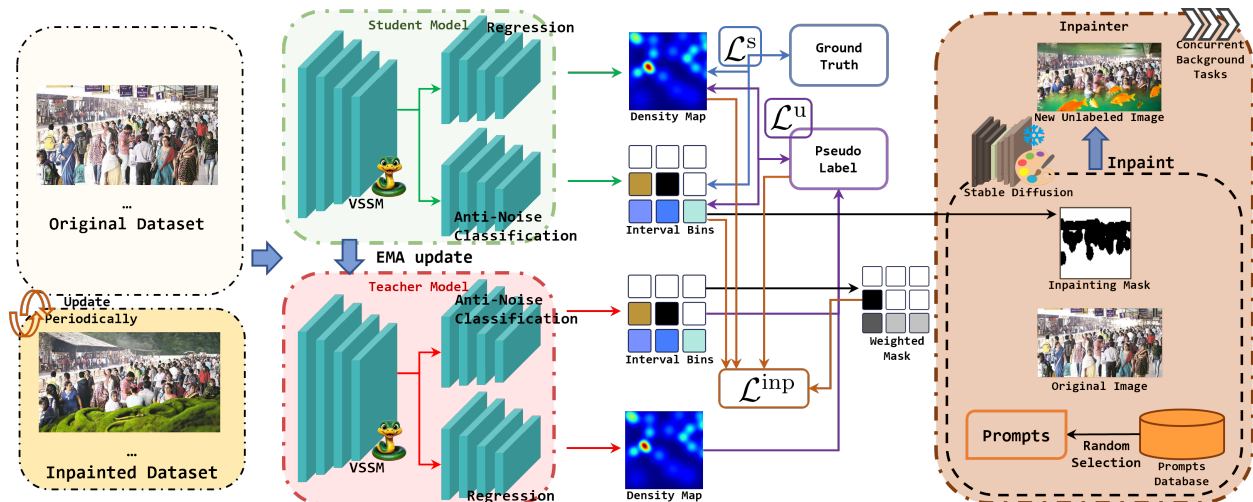


Figure 2. The overall framework of our method TMTB. TMTB contains the Mean Teacher framework for semi-supervised learning, VSSM as the backbone, a classification branch for predicting masks, and an inpainter for inpainting augmentation. The inpainting process is conducted periodically, which generates or updates the inpainted images. For filtering out unreliable regions, the teacher model generates the weighted mask based on the inconsistency level of the inpainted image, which is applied in  $\mathcal{L}^{\text{inp}}$ . The teacher model generates pseudo-labels for unlabeled data (inpainted images included), and the student model predicts on labeled data and strongly augmented unlabeled data (inpainted images included).

tially [23] based on Transformers, which are weak in modeling long-range dependencies. When facing extremely dense crowd scenes, the performance of these methods is not satisfactory.

**Generative Data Augmentation.** Deep learning models tend to overfit when the quantity of data is limited, which harms the generalization ability of models. Therefore, data augmentation was proposed to address this issue. For image-based tasks, basic data augmentation methods include random cropping, flipping, rotation, scaling, color jittering, and noise adding. Some advanced data augmentation methods, such as CutMix [62], Mixup [65], and AutoAugment [7], have been proposed. However, these methods are not suitable for crowd counting tasks. Both the density-based and point-based crowd counting methods are sensitive to the spatial structure of the crowd, and the above methods may destroy the spatial structure of the crowd. The damage to the integrity of the crowd will lead to a decrease in model performance. We study this in Table 2.

Generative Data Augmentation [11, 15, 16, 20, 40] is the process of creating new synthetic data points that can be added to existing datasets. This unique approach is widely used to improve the performance of models by increasing the quantity and diversity of training data while maintaining the quality of the data. In [66], queries-only data was used to improve the multilingual task, showing the effectiveness of generative data augmentation. FreeMask [58] resorted to synthetic images from generative models to ease the burden of both data collection and annotation procedures, and achieves comparable performance to real-data-based meth-

ods. G-DAUG<sup>C</sup> [59] generated synthetic examples using pretrained language models, and selects the most informative and diverse set of examples for data augmentation, to achieve more accurate and robust learning in low-resource setting. DiffusionMix [18] employed an inpaint-and-mix strategy to generate label-preserved data for classification task. However, it requires pre-defined binary masks to concatenate the original and generated images, which is not available in crowd counting since the position and shape of the crowd are unpredictable. Compared to existing works, our contribution is to fill the gap in effective augmentation methods within the field of pixel-level prediction tasks.

### 3. Method

We propose a semi-supervised crowd counting method that enhances the dataset using a diffusion-based model’s inpainting technique and utilizes a VSSM (Visual State Space Model) with Anti-Noise classification branch to improve data diversity and model performance.

The overall framework of our method, TMTB, is shown in Figure 2. Our method is built on the Mean Teacher framework, which is widely employed in semi-supervised learning. The teacher model shares the same architecture as the student model, and its weights are updated using the student model’s weights through the Exponential Moving Average (EMA) strategy. VMamba [29], a novel VSSM (Visual State Space Model), serves as the backbone, replacing the CNN and Transformer. The image features extracted from VMamba are then fed into two independent branches: the counting branch and the classification branch, for pre-

dictions. The counting branch predicts a density map of the image, while the classification branch predicts the indices of pre-defined count interval bins. We build a module, Inpainter, designed to periodically applying background inpainting augmentation to the training set.

We first describe our novel inpainting augmentation in Section 3.1, then we discuss our network architecture in Section 3.2, and finally, we present our loss functions in Section 3.3.

### 3.1. Inpainting Augmentation

Unlike classification or regression tasks, the ground truth density maps are generated by point-level annotations. The state-of-the-art data augmentation techniques, Mixup [65], CutMix [62], BCP [2], etc., are not applicable to crowd counting, since the augmentation may cause damage to ground truth density maps. We introduce the inpainting technique of diffusion-based models [15, 43] as a novel data augmentation method with the filtering capability of unreliable regions, which generates new samples, thereby expanding the diversity of dataset.

For the inpainting mask  $M^{\text{inp}}$ , the count interval bins predicted by the classification branch are used to separate the foreground and the background of image  $x$ . We generate the positive text prompt randomly to achieve more diverse unlabeled dataset, but the negative text prompt is kept the same for all samples. The inpainting process is conducted periodically during the training process using a preset time interval  $T^{\text{inp}}$ :

$$\begin{aligned} M^{\text{inp}} &= \mathbf{0}(\arg \max(\hat{p})), \\ x^{\text{inp}} &= \mathcal{SD}(x, M^{\text{inp}}, r^{\text{pos}}, r^{\text{neg}}), \end{aligned} \quad (1)$$

where  $\hat{p}_i$  is the predicted probability distribution from the classification branch,  $\mathbf{0}(\cdot)$  is the indicator function,  $x^{\text{inp}}$  is the new image with the background inpainted,  $\mathcal{SD}(\cdot, \cdot, \cdot, \cdot)$  represents Stable Diffusion [43], which is a mature, excellent, and cost-effective diffusion model, and  $r^{\text{pos}}$  and  $r^{\text{neg}}$  are the positive and negative text prompts, respectively.

Figure 3 shows examples of both good and poor inpainting samples. All new samples are considered unlabeled, as the inpainting process may add additional humans for better coherence. For well-inpainted samples, the foreground regions are well preserved, while the background regions are inpainted with different patterns, thus introducing diversity to the dataset. Even though the inpainting process is not perfect, the model can still benefit from the augmented dataset. However, failures may sometimes occur, potentially leading to the model learning from noisy inputs. The heads of humans and other features in the unreliable regions of poorly-inpainted images are fragmented and indistinct, rendering them difficult to recognize. It is necessary to **filter out** these **unreliable regions**. The EMA model calculates



Figure 3. Inpainting samples. The left part shows well-inpainted couples, while the right part shows poorly-inpainted couples. Column (a) and (c) are the original images, while column (b) and (d) are the inpainted images.

the inconsistency level of the inpainted image by the difference in the classification branch between the weakly augmented version and the strongly augmented version. The inconsistency level and the weighted mask are defined as follows:

$$\begin{aligned} M_l^{\text{incon}} &= \mathbf{0}(|\hat{p}^s - \hat{p}^w| - l), \\ \omega_l^t &= \text{softmax}\left(e^{-l \cdot t / T^{\text{inp}w}}\right), \\ M^{\text{incon}} &= \sum_{l=0}^L M_l^{\text{incon}} \cdot \omega_l^t, \end{aligned} \quad (2)$$

where  $\hat{p}^s$  and  $\hat{p}^w$  are the predicted probability distributions of the classification branch of EMA model in the strong and weak augmentation version, respectively.  $M_l^{\text{incon}}$  is the mask of inconsistency level  $l$ ,  $M^{\text{incon}}$  is the final weighted mask,  $\omega_l^t$  is the weight of inconsistency level  $l$  at time  $t$ ,  $T^{\text{inp}w}$  is the parameter controlling the weight decay speed, and  $L$  is the number of inconsistency levels. The  $L$  depends on the predefined count interval bins, and since we followed the interval bins settings in [54], the  $L$  is set to 2 for the balance of diversity and reliability. The weighted mask is then used to adjust the loss associated with the inpainted image.

### 3.2. VSSM with Classification for Anti-Noise

**Visual State Space Models (VSSMs).** Existing crowd counting methods often encounter challenges such as congestion, blur, and occlusion in intricate scenes. CNN-based approaches tend to overfit to local details, while Transformer-based methods excel in global modeling but face heavy computational burdens due to their quadratic complexity in terms of image sizes. These limitations motivate us to introduce the VSSM, which captures comprehensive long-range information with linear time complexity, for the crowd counting task.

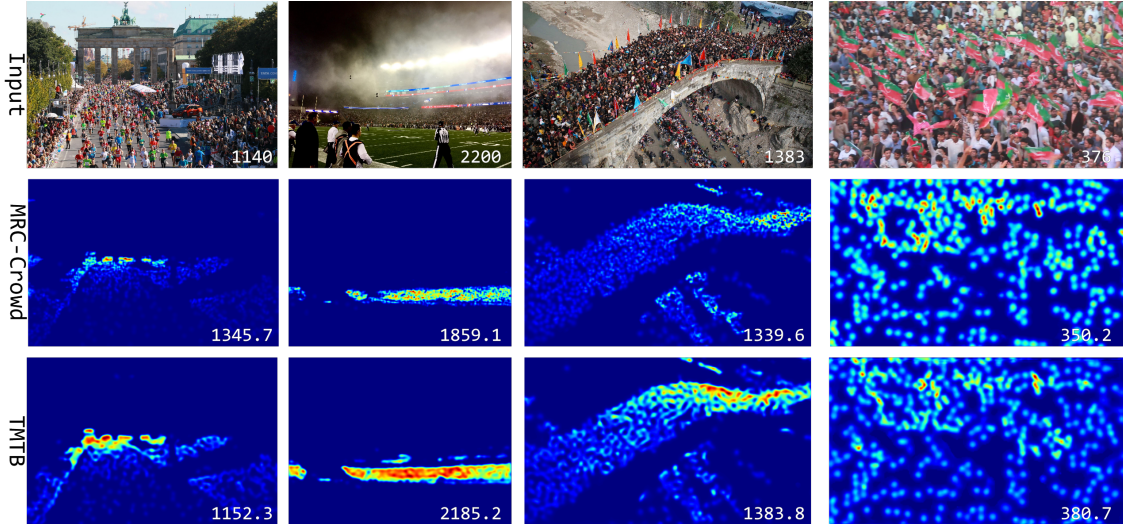


Figure 4. Visualizations of the predictions on the test set of the JHU-Crowd++ dataset. The first row shows the input images. The second row displays the predictions of the SOTA method MRC-Crowd [39]. The third row presents the predictions of our method TMTB. All models are trained with 5% labeled data.

State Space Models (SSMs) map the input stimulation  $u(t)$  to the output response  $y(t)$  by means of a hidden state  $h(t)$ . These processes are formulated with the following form:

$$\begin{aligned} h'(t) &= Ah(t) + Bu(t), \\ y(t) &= Ch(t) + Du(t), \end{aligned} \quad (3)$$

where  $A$ ,  $B$ ,  $C$ , and  $D$  are the weighting parameters.

Linear time-invariant SSMs (Equation (3)) lack the ability to capture the contextual information, [12] proposed a novel parameterization method for SSMs that integrates an input-dependent selection mechanism (referred to as S6). VMamba [29] replaces the S6 module, with the newly proposed 2D-Selective-Scan (SS2D) module which concurrently achieving global receptive fields, dynamic weights, and linear complexity. By adopting complementary 1D traversal paths, SS2D enables each pixel in the image to effectively integrate information from all other pixels in different directions, thereby facilitating the establishment of global receptive fields in the 2D space and generating more accurate density map. Details about the SS2D module could be found in [29]. The features extracted by the final SS2D block are then fed into two branches: one for density map regression and the other for count interval classification, which is designed for less inexact and more accurate supervision.

**Exact: Regression Head.** The regression head is designed to predict the density map for the input image. The density map is then summed to obtain the exact final count value. The regression head consists of up-sampling layers, convolutional layers, batch normalization layers, and ReLU activation layers. We followed MRC-Crowd [39] employing the loss function proposed in CUT [38], which significantly

boosts the performance in the foreground area. It could be expressed as:

$$\begin{aligned} \mathcal{L}_{\text{reg}} &= \frac{1}{J} \sum_{j=1}^J (1 - \text{SSIM}(D_j(\hat{y} \odot M^{gt})), \\ &D_j(y^{gt} \odot M^{gt}))) + \alpha \cdot \mathcal{L}_{TV}(\hat{y}, y^{gt}), \end{aligned} \quad (4)$$

where  $\text{SSIM}(\cdot, \cdot)$  is the structural similarity index measure, and  $D_j$  denotes the average pooling operation that down-samples an image to  $1/2^j$  of its original size. The operation  $\odot$  denotes the Hadamard product, and  $M^{gt}$  is the binary mask that distinguishes the dense and sparse regions based on a predefined threshold  $\tau$ . It can be obtained using the indicator function  $\mathbf{1}$  as  $M^{gt} = \mathbf{1}(y^{gt} > \tau)$ .  $\alpha$  is a hyperparameter that balances the two terms.  $J$  and  $\alpha$  are set to 3 and 0.01, respectively.  $\mathcal{L}_{TV}$  is the total variation loss.

**Accurate: Anti-Noise Classification Head.** Many previous works [1, 31, 34, 53] have identified the problem of inaccurate ground truth annotations in crowd counting datasets, which render the ground truth density maps noisy and inaccurate. In this way, the model may learn from the noisy ground truth and generate inaccurate density maps. Inspired by previous works [23, 39, 54], we employ the Anti-Noise classification task as an auxiliary task, which is more robust in predicting inexact and accurately. The Anti-Noise classification branch is supervised by the inexact but accurate count interval bins rather than the exact but maybe inaccurate density maps. Furthermore, we use the prediction of the this branch to generate reliable masks for inpainting samples, and we discuss this in Section 3.1. The goal of the Anti-Noise classification branch is to predict the accurate count interval bins, which are predefined by [54].

The Anti-Noise classification head consists of an up-

sampling layer, a convolutional layer, a ReLU activation layer and a final convolutional layer. The standard cross-entropy loss is applied. In the case of labeled data, the loss is defined as:

$$\mathcal{L}_{\text{cls}} = \frac{1}{N} \sum_i \mathcal{H}(p_i^{gt}, \hat{p}_i), \quad (5)$$

where  $\mathcal{H}$  is the cross-entropy loss function,  $p_i^{gt}$  is the ground truth probability distribution, and  $\hat{p}_i$  is the predicted probability distribution.

### 3.3. Losses

In order to make full use of the labeled data  $L = \{(x_i^l, DM_i^{gt})\}_{i=1}^{N_l}$  and unlabeled data  $U = \{(x_i^u)\}_{i=1}^{N_u}$ , we employ a common semi-supervised learning strategy widely used in crowd counting. The labeled samples are used to directly train the student model, while the unlabeled samples are used for consistency regularization. For labeled data, the supervised loss  $\mathcal{L}^s = \mathcal{L}_{\text{reg}}^s + \mathcal{L}_{\text{cls}}^s$  is a combination of the regression loss (Equation (4)) and the classification loss (Equation (5)). Given the absence of a confidence score for the predicted regression map, we choose to apply consistency regularization to all unlabeled samples, rather than developing an algorithm to assess prediction uncertainty. The EMA teacher model generates pseudo-labels based on the prediction of unlabeled data with weak augmentation. The student model makes predictions based on the strong augmentation version. The error loss between the two predictions is calculated as the consistency loss.

Despite the common strong augmentation, we also introduce a patch-aligned random masking strategy [57] as a kind of strong augmentation. The patch-aligned random masking strategy randomly masks out some patches of various sizes in the image. The student model is required to predict based on masked images, while the teacher model is able to access the full image. The semi-supervised loss is defined as:

$$\mathcal{L}^u = \text{MAE}(\hat{y}^{st}, \hat{y}^{ema}) + \text{MAE}(\hat{p}^{st}, \hat{p}^{ema}), \quad (6)$$

where  $\hat{y}^{st}$  and  $\hat{y}^{ema}$  are the predicted density maps of the student model and the teacher model, respectively.  $\hat{p}^{st}$  and  $\hat{p}^{ema}$  are the predicted count interval bins of the student model and the teacher model, respectively.

Consistency loss is also applied to the inpainted images. However, to avoid the model learning from noisy regions with low quality, the loss is adjusted by the weighted mask of inconsistency level. The inpainting loss is defined as:

$$\mathcal{L}^{\text{inp}} = M^{\text{incon}} \times \text{MAE}(\hat{y}^{st}, \hat{y}^{ema}) + M^{\text{incon}} \times \text{MAE}(\hat{p}^{st}, \hat{p}^{ema}), \quad (7)$$

where  $M^{\text{incon}}$  is the weighted mask of inconsistency level mentioned in Equation (2).

The final loss is a combination of the supervised, semi-supervised, and inpainting losses:

$$\mathcal{L} = \mathcal{L}^s + \lambda_w \cdot \mathcal{L}^u + \lambda_w \cdot \mathcal{L}^{\text{inp}}, \quad (8)$$

where  $\lambda_w$  is the warm-up weight for the semi-supervised loss and the inpainting loss.

## 4. Experiments

We evaluate our method on four public datasets:

- **JHU-Crowd++** [46] is a comprehensive dataset with 4,372 images and 1.51 million annotations, collected under a variety of scenarios and environmental conditions.
- **UCF-QNRF** [17] contains 1535 images. The dataset has a greater number of high-count crowd images and annotations, and a wider variety of scenes containing the most diverse set of viewpoints, densities and lighting variations.
- **ShanghaiTech A & B** [68] are two datasets containing nearly 1,200 images and 330,000 labeled heads.

To achieve fair comparisons, we follow the same semi-supervised experimental protocol as previous works [23, 24, 39], including the 5%, 10%, and 40% labeled data settings and the split of labeled and unlabeled data. The evaluation metrics are Mean Absolute Error (MAE) and Root Mean Squared Error (RMSE). The detailed definitions of them are provided in the supplementary material.

For some excessively high-resolution images, we scale them down, ensuring the longest side does not exceed 1,920 pixels. For the ground truth density map, we use geometry-adapted Gaussian kernels described in [22] for all datasets except the ShanghaiTech B dataset, and we fix the size of the kernel to 4. When training, the input images are randomly cropped to  $512 \times 512$  pixels for all datasets except for ShanghaiTech A. The inputs from ShanghaiTech A are cropped to  $256 \times 256$  pixels instead. The count interval bins, which should be predicted by the classification branch, are set to the same as those in [54]. The AdamW optimizer [30] with a learning rate of  $10^{-5}$  is used to optimize the model. The weight decay is set to  $10^{-4}$ . The downsample factor is set to 8. The batch size is set to 8. In 5% and 10% labeled data settings, the ratio of labeled data to unlabeled data is set to 2 : 6. In the 40% labeled data setting, the ratio is set to 4 : 4. As we mentioned in Section 3.3, we use the patch-aligned random masking strategy [57] as a form of strong augmentation. The masked patch size and the masked region ratio are set to  $32 \times 32$  and 0.3, respectively. The ablation details can be found in [39]. The teacher model is updated by the exponential moving average with a decay rate of 0.97. The weights of all losses are set to 1.0. For  $\mathcal{L}^u$  and  $\mathcal{L}^{\text{inp}}$ , we ramp the weights from 0 to 1.0 in the first 20 epochs. The max accepted inconsistency level  $L$  is set to 2, and the hyperparameter  $T^{\text{inp}w}$  is set to 100. The ablation study of  $T^{\text{inp}w}$  is conducted in Section 4.2. Each training

Table 1. Comparisons with the SOTA methods on main public datasets. The best results are highlighted in bold, and the second-best results are underlined.

Methods	Venue	Labeled Percentage	JHU-Crowd++		UCF-QNRF		ShanghaiTech A		ShanghaiTech B	
			MAE ↓	RMSE ↓	MAE ↓	RMSE ↓	MAE ↓	RMSE ↓	MAE ↓	RMSE ↓
MT [51]	NIPS'17	5%	101.5	363.5	172.4	284.9	104.7	156.9	19.3	33.2
L2R [26]	CVPR'18	5%	101.4	338.8	160.1	272.3	103.0	155.4	20.3	27.6
DACount [23]	ACM MM'22	5%	82.2	294.9	120.2	209.3	85.4	134.5	12.6	22.8
OT-M [24]	CVPR'23	5%	82.7	304.5	118.4	195.4	83.7	133.3	12.6	21.5
MRC-Crowd [39]	T-CSVT'24	5%	<u>76.5</u>	<u>282.7</u>	<u>101.4</u>	<u>171.3</u>	74.8	<b>117.3</b>	<u>11.7</u>	<b>17.8</b>
<b>TMTB</b>	<b>Ours</b>	5%	<b>67.0</b>	<b>252.2</b>	<b>96.3</b>	<b>163.4</b>	<b>72.4</b>	<u>126.4</u>	<b>10.6</b>	<u>19.6</u>
MT [51]	NIPS'17	10%	90.2	319.3	145.5	250.3	94.5	156.1	15.6	24.5
L2R [26]	CVPR'18	10%	87.5	315.3	148.9	249.8	90.3	153.5	15.6	24.4
DACount [23]	ACM MM'22	10%	75.9	282.3	109.0	187.2	74.9	115.5	11.1	19.1
MTCP [72]	T-NNLS'23	10%	88.1	318.7	124.7	206.3	81.3	130.5	14.5	22.3
OT-M [24]	CVPR'23	10%	73.0	280.6	113.1	186.7	80.1	118.5	10.8	18.2
CU [21]	ICCV'23	10%	74.9	281.7	104.0	164.3	70.8	116.6	<b>9.7</b>	17.7
SALCrowd [67]	ACM MM'24	10%	<u>69.7</u>	<u>263.5</u>	106.7	171.3	69.7	114.5	<b>9.7</b>	<u>17.5</u>
MRC-Crowd [39]	T-CSVT'24	10%	70.7	<b>261.3</b>	<u>93.4</u>	<b>153.2</b>	<u>67.3</u>	<b>106.8</b>	10.3	18.2
<b>TMTB</b>	<b>Ours</b>	10%	<b>66.3</b>	265.1	<b>91.7</b>	<u>156.3</u>	<b>65.7</b>	<u>110.4</u>	<u>9.8</u>	<b>17.2</b>
MT [51]	NIPS'17	40%	121.5	388.9	147.2	247.6	88.2	151.1	15.9	25.7
L2R [26]	CVPR'18	40%	123.6	376.1	145.1	256.1	86.5	148.2	16.8	25.1
SUA [33]	ICCV'21	40%	80.7	290.8	130.3	226.3	68.5	121.9	14.1	20.6
DACount [23]	ACM MM'22	40%	65.1	260.0	91.1	153.4	67.5	110.7	9.6	14.6
OT-M [24]	CVPR'23	40%	72.1	272.0	100.6	167.6	70.7	114.5	8.1	13.1
SALCrowd [67]	ACM MM'24	40%	<u>62.0</u>	255.1	95.0	167.0	<b>60.7</b>	<u>97.2</u>	7.9	<b>12.7</b>
MRC-Crowd [39]	T-CSVT'24	40%	<b>60.0</b>	<b>227.3</b>	<b>81.1</b>	<b>131.5</b>	62.1	<b>95.5</b>	<u>7.8</u>	13.3
<b>TMTB</b>	<b>Ours</b>	40%	<b>60.0</b>	<u>240.3</u>	<u>81.4</u>	<u>140.6</u>	<u>60.8</u>	99.0	<b>7.5</b>	<u>12.9</u>

process coordinates with two inpainting background processes. The inpainting period  $T^{\text{inp}}$  is set to 80 epochs.

#### 4.1. Main Results

In our main experiments, the proposed TMTB demonstrates superior performance compared to state-of-the-art methods across four public datasets with three labeled data percentages. The results are shown in Table 1.

Notably, when utilizing only 5% labeled data, TMTB achieves the lowest MAEs of 67.0 on JHU-Crowd++, 96.3 on UCF-QNRF, 72.4 on ShanghaiTech A, and 10.6 on ShanghaiTech B, demonstrating the best performance. The result on JHU-Crowd++ not only surpasses the performance of SOTA methods with the same amount of labeled data but also demonstrates that TMTB remains superior even at the 10% label setting, highlighting its efficient label utilization and exceptional accuracy. With a 10% labeled data setting, TMTB continues to outstand, obtaining a leading MAE of 66.3 on JHU-Crowd++, 91.7 on UCF-QNRF, and 65.7 on ShanghaiTech A, further demonstrating its generalization ability and effectiveness. At 40% labeled data, TMTB achieves competitive results, matching the lowest MAE of 60.0 on JHU-Crowd++, and decreasing the MAE to a lowest of 7.5 on ShanghaiTech B, maintaining strong performance across the other datasets. These results underscore the capability of TMTB to achieve low error with minimal labeled data, offering substantial improvements over SOTA methods.

Table 2. An study of common various augmentation strategies on ShanghaiTech-A dataset using 10% labeled data.

Augmentation	MAE ↓	RMSE ↓
Mixup [65]	285.16	431.83
Mixup [65] (background only)	72.00	116.85
CutMix [62]	312.60	462.33
BCP [2]	70.99	121.83
<b>TMTB (Ours)</b>	65.74	110.42

**Augmentation Strategies.** In order to investigate the effectiveness of the proposed inpainting augmentation strategy, we compare it with some off-the-shelf augmentation strategies, on the ShanghaiTech A dataset with 10% labeled data, including Mixup [65], CutMix [62], and BCP [2]. The results are shown in Table 2.

Mixup and CutMix both degrade the performance when applied to the whole image. The main reason is that the integrity of the foreground and background regions is destroyed, making the augmented images non-informative and hard to learn. These results demonstrate the importance of the integrity of the foreground and background regions in the crowd counting task. We then apply Mixup to the background region only, and the performance improves. This approach is somewhat similar to the inpainting augmentation, which enhances the background region while keeping the foreground region intact. However, the background regions are sampled from the domain of the original dataset, which

Table 3. Comparisons with SOTA single domain generalization methods on Q (UCF-QNRF) and A (ShanghaiTech-A) datasets. The best results are highlighted in bold, and the second-best results are underlined.

Methods	Venue	Source Labeled Percentage	A → Q		Q → A	
			MAE ↓	RMSE ↓	MAE ↓	RMSE ↓
IBN [35]	ECCV'18	100%	280.2	561.0	105.9	174.6
SW [36]	ICCV'19	100%	285.5	431.0	102.4	168.8
ISW [6]	CVPR'21	100%	215.6	399.7	83.4	136.0
DG-MAN [32]	ICCV'21	100%	129.1	238.2	-	-
DCCUS [9]	AAAI'23	100%	119.4	216.6	67.4	112.8
MPCount [37]	CVPR'24	100%	<u>115.7</u>	<u>199.8</u>	<u>65.5</u>	<u>110.1</u>
<b>TMTB</b>	<b>Ours</b>	40%	<b>112.5</b>	<b>190.6</b>	<b>62.4</b>	<b>103.5</b>

Table 4. Comparisons with SOTA domain adaptation methods on Q (UCF-QNRF) and A (ShanghaiTech-A) datasets. The best results are highlighted in bold, and the second-best results are underlined.

Methods	Venue	Source Labeled Percentage	Target Domain Visible	A → Q		Q → A	
				MAE ↓	RMSE ↓	MAE ↓	RMSE ↓
RBT [28]	ACM MM'20	100%	✓	175.0	294.8	-	-
C <sup>2</sup> MoT [56]	ACM MM'21	100%	✓	125.7	218.3	-	-
FGFD [69]	ACM MM'22	100%	✓	124.1	242.0	70.2	118.4
DAOT [70]	ACM MM'23	100%	✓	113.9	215.6	67.0	128.4
FSIM [71]	T-MM'23	100%	✓	<b>105.3</b>	<u>191.1</u>	<u>66.8</u>	<u>111.5</u>
<b>TMTB</b>	<b>Ours</b>	40%	✗	<u>112.5</u>	<b>190.6</b>	<b>62.4</b>	<b>103.5</b>

may not be sufficiently diverse. BCP is a recent birectical augmentation strategy designed for medical image segmentation. We employ it in the crowd counting task and find it can also improve the performance. However, the performance is not competitive enough when compared to SOTA methods.

**Domain Generalization & Domain Adaptation.** We compare our method with state-of-the-art single domain generalization methods and obtain remarkable results in Table 3. The results show that our method outperforms the SOTA methods on both UCF-QNRF → ShanghaiTech-A and ShanghaiTech-A → UCF-QNRF tasks, utilizing only 40% labeled data on the source domain instead of 100%. Note that IBN, SW, and ISW are originally designed for image classification or segmentation, and are adapted to crowd counting and reported by MPCount [37]. The results demonstrate the effectiveness of VSSM and inpainting augmentation in our method.

The study on domain adaptation is also conducted, and the results are shown in Table 4. Domain adaptation setting is easier than domain generalization, as the target domain is visible. It is surprising that our method achieves competitive results compared to SOTA methods, even though we only have 40% labeled data available in the source domain and no access to the target domain. The comparisons again provide evidence of the generalization ability of TMTB.

Table 5. An ablation study on the effectiveness of various components on UCF-QNRF dataset using 5% labeled data.

VSSM	$\mathcal{L}^s$	$\mathcal{L}^u$	$\mathcal{L}^{inp}$	MAE ↓	RMSE ↓
✗	$\mathcal{L}_{reg}^s$			115.35	188.19
✓	$\mathcal{L}_{reg}^s$			110.41	185.52
✓	$\mathcal{L}_{reg}^s + \mathcal{L}_{cls}^s$			105.88	183.87
✓	$\mathcal{L}_{reg}^s + \mathcal{L}_{cls}^s$		✓	103.58	178.97
✓	$\mathcal{L}_{reg}^s + \mathcal{L}_{cls}^s$		✓ $\omega_l$	97.21	166.06
✓	$\mathcal{L}_{reg}^s + \mathcal{L}_{cls}^s$		✓ $\omega_l^t$	96.33	163.42

## 4.2. Ablation Study

**Components.** We conduct an ablation study to analyze the effectiveness of various components in our method on the UCF-QNRF dataset with 5% labeled data. The results are shown in Table 5. The VSSM is the core component. Compared to OT-M [24], the VSSM with supervised loss  $\mathcal{L}^s$  improves the performance by decreasing the MAE by 10.57%. After adding the semi-supervised loss  $\mathcal{L}^u$ , the performance is further improved, showing the effectiveness of our semi-supervised learning strategy. Next, we introduce our novel inpainting augmentation strategy and its mask of inconsistency level  $M_l^{incon}$  but with fixed weights  $\omega_l$ . The performance is further improved, and the MAE of 97.21 surpasses the SOTA method MRC-Crowd [39] at 101.4. Finally, we employ time-based weights  $\omega_l^t$  for the inpainting loss, and the performance is significantly improved, achieving the lowest MAE of 96.33 and RMSE of 163.42.

**Weight Decay Speed.** We study the impact of the weight decay speed  $T^{inpw}$  on the JHU-Crowd++ dataset with 5% labeled data. The detailed influence of  $T^{inpw}$  on the MAE and RMSE is shown in supplementary material. We train and test TMTB with different  $T^{inpw}$  values ranging from 80 to 120. The results show that both MAE and RMSE decrease as  $T^{inpw}$  increases from 80 to 100. However, when  $T^{inpw}$  is greater than 100, the performance begins to degrade. Therefore, we set  $T^{inpw}$  to 100 in experiments.

## 5. Conclusion

In the literature of semi-supervised crowd counting, a number of methods based on pseudo-labeling have been explored. Despite their success, these methods still struggle to achieve satisfactory performance in extremely crowded, low-light, and adverse weather scenarios. In this work, we reveal that the lack of suitable data augmentation methods and the weakness of capturing global context information are bottlenecks. Therefore, we design a novel inpainting augmentation method, Inpainting Augmentation that works better for crowd counting, enabling tasting more. Moreover, we introduce the Visual State Space Model to capture long-range dependencies in crowd counting, enabling tasting better. Our proposed framework, TMTB, achieves superior performance compared to existing methods.

## References

- [1] Shuai Bai, Zhiqun He, Yu Qiao, Hanzhe Hu, Wei Wu, and Junjie Yan. Adaptive dilated network with self-correction supervision for counting. In *Proceedings of the IEEE/CVF Conference on Computer Vision and Pattern Recognition (CVPR)*, 2020. 5
- [2] Yunhao Bai, Duowen Chen, Qingli Li, Wei Shen, and Yan Wang. Bidirectional copy-paste for semi-supervised medical image segmentation. In *Proceedings of the IEEE/CVF Conference on Computer Vision and Pattern Recognition (CVPR)*, pages 11514–11524, 2023. 2, 4, 7
- [3] Lokesh Boominathan, Srinivas S S Kruthiventi, and R. Venkatesh Babu. Crowdnet: A deep convolutional network for dense crowd counting. In *Proceedings of the 24th ACM International Conference on Multimedia*, page 640–644, New York, NY, USA, 2016. Association for Computing Machinery. 1
- [4] Olivier Chapelle, Jason Weston, Léon Bottou, and Vladimir Vapnik. Vicinal risk minimization. In *Advances in Neural Information Processing Systems*. MIT Press, 2000. 2
- [5] Lei Chen, Xinghang Gao, Fei Chao, Xiang Chang, Chih Min Lin, Xingen Gao, Shaopeng Lin, Hongyi Zhang, and Juqiang Lin. The effectiveness of a simplified model structure for crowd counting, 2024. 2
- [6] Sungha Choi, Sanghun Jung, Huiwon Yun, Joanne T. Kim, Seungryoung Kim, and Jaegul Choo. Robustnet: Improving domain generalization in urban-scene segmentation via instance selective whitening. In *Proceedings of the IEEE/CVF Conference on Computer Vision and Pattern Recognition (CVPR)*, pages 11580–11590, 2021. 8
- [7] Ekin D. Cubuk, Barret Zoph, Dandelion Mane, Vijay Vasudevan, and Quoc V. Le. Autoaugment: Learning augmentation strategies from data. In *Proceedings of the IEEE/CVF Conference on Computer Vision and Pattern Recognition (CVPR)*, 2019. 3
- [8] Weihang Dai, Xiaomeng Li, and Kwang-Ting Cheng. Semi-supervised deep regression with uncertainty consistency and variational model ensembling via bayesian neural networks. *Proceedings of the AAAI Conference on Artificial Intelligence*, 37(6):7304–7313, 2023. 2
- [9] Zhipeng Du, Jiankang Deng, and Miaoqing Shi. Domain-general crowd counting in unseen scenarios. *Proceedings of the AAAI Conference on Artificial Intelligence*, 37(1):561–570, 2023. 8
- [10] Yue Duan, Zhen Zhao, Lei Qi, Lei Wang, Luping Zhou, Yinghuan Shi, and Yang Gao. Mutexmatch: Semi-supervised learning with mutex-based consistency regularization. *IEEE Trans. Neural Networks Learn. Syst.*, 35(6): 8441–8455, 2024. 2
- [11] Ian Goodfellow, Jean Pouget-Abadie, Mehdi Mirza, Bing Xu, David Warde-Farley, Sherjil Ozair, Aaron Courville, and Yoshua Bengio. Generative adversarial networks. *Communications of the ACM*, 63(11):139–144, 2020. 3
- [12] Albert Gu and Tri Dao. Mamba: Linear-time sequence modeling with selective state spaces. In *First Conference on Language Modeling*, 2024. 5
- [13] Tao Han, Lei Bai, Lingbo Liu, and Wanli Ouyang. Steerer: Resolving scale variations for counting and localization via selective inheritance learning. In *Proceedings of the IEEE/CVF International Conference on Computer Vision (ICCV)*, pages 21848–21859, 2023. 2
- [14] Marcus Handte, Muhammad Umer Iqbal, Stephan Wagner, Wolfgang Apolinarski, Pedro José Marrón, Eva Maria Muñoz Navarro, Santiago Martínez, Sara Izquierdo Barthelemy, and Mario González Fernández. Crowd density estimation for public transport vehicles. In *EDBT/ICDT Workshops*, pages 315–322. Citeseer, 2014. 1
- [15] Jonathan Ho, Ajay Jain, and Pieter Abbeel. Denoising diffusion probabilistic models. In *Advances in Neural Information Processing Systems*, pages 6840–6851. Curran Associates, Inc., 2020. 3, 4
- [16] Jonathan Ho, Ajay Jain, and Pieter Abbeel. Denoising diffusion probabilistic models. *Advances in neural information processing systems*, 33:6840–6851, 2020. 3
- [17] Haroon Idrees, Muhmmad Tayyab, Kishan Athrey, Dong Zhang, Somaya Al-Maadeed, Nasir Rajpoot, and Mubarak Shah. Composition loss for counting, density map estimation and localization in dense crowds. In *Proceedings of the European conference on computer vision (ECCV)*, pages 532–546, 2018. 1, 2, 6
- [18] Khawar Islam, Muhammad Zaigham Zaheer, Arif Mahmood, and Karthik Nandakumar. Diffusemix: Label-preserving data augmentation with diffusion models. In *Proceedings of the IEEE/CVF Conference on Computer Vision and Pattern Recognition (CVPR)*, pages 27621–27630, 2024. 3
- [19] Neal Jean, Sang Michael Xie, and Stefano Ermon. Semi-supervised deep kernel learning: Regression with unlabeled data by minimizing predictive variance. In *Advances in Neural Information Processing Systems*. Curran Associates, Inc., 2018. 2
- [20] Diederik P Kingma. Auto-encoding variational bayes. *arXiv preprint arXiv:1312.6114*, 2013. 3
- [21] Chen Li, Xiaoling Hu, Shahira Arousamra, and Chao Chen. Calibrating uncertainty for semi-supervised crowd counting. In *2023 IEEE/CVF International Conference on Computer Vision (ICCV)*, pages 16685–16695, 2023. 1, 2, 7
- [22] Yuhong Li, Xiaofan Zhang, and Deming Chen. Csrnet: Dilated convolutional neural networks for understanding the highly congested scenes. In *Proceedings of the IEEE Conference on Computer Vision and Pattern Recognition (CVPR)*, 2018. 6
- [23] Hui Lin, Zhiheng Ma, Xiaopeng Hong, Yaowei Wang, and Zhou Su. Semi-supervised crowd counting via density agency. In *Proceedings of the 30th ACM International Conference on Multimedia*, page 1416–1426, New York, NY, USA, 2022. Association for Computing Machinery. 2, 3, 5, 6, 7
- [24] Wei Lin and Antoni B. Chan. Optimal transport minimization: Crowd localization on density maps for semi-supervised counting. In *Proceedings of the IEEE/CVF Conference on Computer Vision and Pattern Recognition (CVPR)*, pages 21663–21673, 2023. 1, 6, 7, 8

- [25] Weizhe Liu, Mathieu Salzmann, and Pascal Fua. Context-aware crowd counting. In *Proceedings of the IEEE/CVF Conference on Computer Vision and Pattern Recognition (CVPR)*, 2019. 1
- [26] Xialei Liu, Joost van de Weijer, and Andrew D. Bagdanov. Leveraging unlabeled data for crowd counting by learning to rank. In *Proceedings of the IEEE Conference on Computer Vision and Pattern Recognition (CVPR)*, 2018. 2, 7
- [27] Yan Liu, Lingqiao Liu, Peng Wang, Pingping Zhang, and Yinjie Lei. Semi-supervised crowd counting via self-training on surrogate tasks. In *Computer Vision—ECCV 2020: 16th European Conference, Glasgow, UK, August 23–28, 2020, Proceedings, Part XV 16*, pages 242–259. Springer, 2020. 2
- [28] Yuting Liu, Zheng Wang, Miaoqing Shi, Shin’ichi Satoh, Qijun Zhao, and Hongyu Yang. Towards unsupervised crowd counting via regression-detection bi-knowledge transfer. In *Proceedings of the 28th ACM International Conference on Multimedia*, page 129–137, New York, NY, USA, 2020. Association for Computing Machinery. 8
- [29] Yue Liu, Yunjie Tian, Yuzhong Zhao, Hongtian Yu, Lingxi Xie, Yaowei Wang, Qixiang Ye, Jianbin Jiao, and Yunfan Liu. VMamba: Visual state space model. In *The Thirty-eighth Annual Conference on Neural Information Processing Systems*, 2024. 3, 5
- [30] Ilya Loshchilov and Frank Hutter. Decoupled weight decay regularization, 2019. 6
- [31] Zhiheng Ma, Xing Wei, Xiaopeng Hong, and Yihong Gong. Bayesian loss for crowd count estimation with point supervision. In *Proceedings of the IEEE/CVF International Conference on Computer Vision (ICCV)*, 2019. 2, 5
- [32] Lucas Mansilla, Rodrigo Echeveste, Diego H. Milone, and Enzo Ferrante. Domain generalization via gradient surgery. In *Proceedings of the IEEE/CVF International Conference on Computer Vision (ICCV)*, pages 6630–6638, 2021. 8
- [33] Yanda Meng, Hongrun Zhang, Yitian Zhao, Xiaoyun Yang, Xuesheng Qian, Xiaowei Huang, and Yalin Zheng. Spatial uncertainty-aware semi-supervised crowd counting. In *Proceedings of the IEEE/CVF International Conference on Computer Vision (ICCV)*, pages 15549–15559, 2021. 7
- [34] Greg Olmschen., Hao Tang., and Zhigang Zhu. Improving dense crowd counting convolutional neural networks using inverse k-nearest neighbor maps and multiscale upsampling. In *Proceedings of the 15th International Joint Conference on Computer Vision, Imaging and Computer Graphics Theory and Applications (VISIGRAPP 2020) - Volume 5: VISAPP*, pages 185–195. INSTICC, SciTePress, 2020. 5
- [35] Xingang Pan, Ping Luo, Jianping Shi, and Xiaoou Tang. Two at once: Enhancing learning and generalization capacities via ibn-net. In *Proceedings of the European Conference on Computer Vision (ECCV)*, 2018. 8
- [36] Xingang Pan, Xiaohang Zhan, Jianping Shi, Xiaoou Tang, and Ping Luo. Switchable whitening for deep representation learning. In *Proceedings of the IEEE/CVF International Conference on Computer Vision (ICCV)*, 2019. 8
- [37] Zhuoxuan Peng and S.-H. Gary Chan. Single domain generalization for crowd counting. In *Proceedings of the IEEE/CVF Conference on Computer Vision and Pattern Recognition (CVPR)*, pages 28025–28034, 2024. 2, 8
- [38] Yifei Qian, Liangfei Zhang, Xiaopeng Hong, Carl Donovan, and Ognjen Arandjelovic. Segmentation assisted u-shaped multi-scale transformer for crowd counting. In *33rd British Machine Vision Conference 2022, BMVC 2022, London, UK, November 21-24, 2022*. BMVA Press, 2022. 5
- [39] Yifei Qian, Xiaopeng Hong, Zhongliang Guo, Ognjen Arandjelović, and Carl R. Donovan. Semi-supervised crowd counting with contextual modeling: Facilitating holistic understanding of crowd scenes. *IEEE Transactions on Circuits and Systems for Video Technology*, 34(9):8230–8241, 2024. 1, 2, 5, 6, 7, 8
- [40] Aditya Ramesh, Mikhail Pavlov, Gabriel Goh, Scott Gray, Chelsea Voss, Alec Radford, Mark Chen, and Ilya Sutskever. Zero-shot text-to-image generation. In *Proceedings of the 38th International Conference on Machine Learning*, pages 8821–8831. PMLR, 2021. 3
- [41] Yasiru Ranasinghe, Nithin Gopalakrishnan Nair, Wele Gedara Chaminda Bandara, and Vishal M. Patel. Crowd-diff: Multi-hypothesis crowd density estimation using diffusion models. In *Proceedings of the IEEE/CVF Conference on Computer Vision and Pattern Recognition (CVPR)*, pages 12809–12819, 2024. 2
- [42] Viresh Ranjan, Hieu Le, and Minh Hoai. Iterative crowd counting. In *Proceedings of the European conference on computer vision (ECCV)*, pages 270–285, 2018. 1
- [43] Robin Rombach, Andreas Blattmann, Dominik Lorenz, Patrick Esser, and Björn Ommer. High-resolution image synthesis with latent diffusion models. In *Proceedings of the IEEE/CVF Conference on Computer Vision and Pattern Recognition (CVPR)*, pages 10684–10695, 2022. 4
- [44] Miaoqing Shi, Zhaohui Yang, Chao Xu, and Qijun Chen. Revisiting perspective information for efficient crowd counting. In *Proceedings of the IEEE/CVF Conference on Computer Vision and Pattern Recognition (CVPR)*, 2019. 1
- [45] Patrice Y. Simard, Yann A. LeCun, John S. Denker, and Bernard Victorri. *Transformation Invariance in Pattern Recognition – Tangent Distance and Tangent Propagation*, pages 235–269. Springer Berlin Heidelberg, Berlin, Heidelberg, 2012. 2
- [46] Vishwanath A. Sindagi, Rajeev Yasarla, and Vishal M. Patel. Jhu-crowd++: Large-scale crowd counting dataset and a benchmark method. *IEEE Transactions on Pattern Analysis and Machine Intelligence*, 44(5):2594–2609, 2022. 2, 6
- [47] Kihyuk Sohn, David Berthelot, Nicholas Carlini, Zizhao Zhang, Han Zhang, Colin A Raffel, Ekin Dogus Cubuk, Alexey Kurakin, and Chun-Liang Li. Fixmatch: Simplifying semi-supervised learning with consistency and confidence. In *Advances in Neural Information Processing Systems*, pages 596–608. Curran Associates, Inc., 2020. 2
- [48] Qingyu Song, Changan Wang, Zhengkai Jiang, Yabiao Wang, Ying Tai, Chengjie Wang, Jilin Li, Feiyue Huang, and Yang Wu. Rethinking counting and localization in crowds: A purely point-based framework. In *Proceedings of the IEEE/CVF International Conference on Computer Vision (ICCV)*, pages 3365–3374, 2021. 2
- [49] Hakki Soy. Edge ai-based crowd counting application for public transport stops. In *Convergence of Deep Learning*

- and *Internet of Things: Computing and Technology*, pages 182–205. IGI Global, 2023. 1
- [50] Aijun Sun, Mao Liu, and Jianfeng Li. Real-time crowd massing risk supervision system based on massing crowd counting in public venue. In *2009 International Symposium on Computer Network and Multimedia Technology*, pages 1–7, 2009. 1
- [51] Antti Tarvainen and Harri Valpola. Mean teachers are better role models: Weight-averaged consistency targets improve semi-supervised deep learning results. *Advances in neural information processing systems*, 30, 2017. 1, 2, 7
- [52] Ashish Vaswani, Noam Shazeer, Niki Parmar, Jakob Uszkoreit, Llion Jones, Aidan N Gomez, Łukasz Kaiser, and Illia Polosukhin. Attention is all you need. In *Advances in Neural Information Processing Systems*. Curran Associates, Inc., 2017. 2
- [53] Jia Wan and Antoni Chan. Adaptive density map generation for crowd counting. In *Proceedings of the IEEE/CVF International Conference on Computer Vision (ICCV)*, 2019. 5
- [54] Changan Wang, Qingyu Song, Boshen Zhang, Yabiao Wang, Ying Tai, Xuyi Hu, Chengjie Wang, Jilin Li, Jiayi Ma, and Yang Wu. Uniformity in heterogeneity: Diving deep into count interval partition for crowd counting. In *Proceedings of the IEEE/CVF International Conference on Computer Vision (ICCV)*, pages 3234–3242, 2021. 4, 5, 6
- [55] Yuchao Wang, Haochen Wang, Yujun Shen, Jingjing Fei, Wei Li, Guoqiang Jin, Liwei Wu, Rui Zhao, and Xinyi Le. Semi-supervised semantic segmentation using unreliable pseudo-labels. In *Proceedings of the IEEE/CVF Conference on Computer Vision and Pattern Recognition (CVPR)*, pages 4248–4257, 2022. 2
- [56] Qiangqiang Wu, Jia Wan, and Antoni B. Chan. Dynamic momentum adaptation for zero-shot cross-domain crowd counting. In *Proceedings of the 29th ACM International Conference on Multimedia*, page 658–666, New York, NY, USA, 2021. Association for Computing Machinery. 8
- [57] Zhenda Xie, Zheng Zhang, Yue Cao, Yutong Lin, Jianmin Bao, Zhuliang Yao, Qi Dai, and Han Hu. Simmim: A simple framework for masked image modeling. In *Proceedings of the IEEE/CVF Conference on Computer Vision and Pattern Recognition (CVPR)*, pages 9653–9663, 2022. 6
- [58] Lihe Yang, Xiaogang Xu, Bingyi Kang, Yinghuan Shi, and Hengshuang Zhao. Freemask: Synthetic images with dense annotations make stronger segmentation models. In *Advances in Neural Information Processing Systems*, pages 18659–18675. Curran Associates, Inc., 2023. 3
- [59] Yiben Yang, Chaitanya Malaviya, Jared Fernandez, Swabha Swayamdipta, Ronan Le Bras, Ji-Ping Wang, Chandra Bhagavatula, Yejin Choi, and Doug Downey. Generative data augmentation for commonsense reasoning. In *Findings of the Association for Computational Linguistics: EMNLP 2020*, pages 1008–1025, Online, 2020. Association for Computational Linguistics. 3
- [60] Jun Yi, Yiran Pang, Wei Zhou, Meng Zhao, and Fujian Zheng. A perspective-embedded scale-selection network for crowd counting in public transportation. *IEEE Transactions on Intelligent Transportation Systems*, 25(5):3420–3432, 2024. 1
- [61] Yingda Yin, Yingcheng Cai, He Wang, and Baoquan Chen. Fishermatch: Semi-supervised rotation regression via entropy-based filtering. In *Proceedings of the IEEE/CVF Conference on Computer Vision and Pattern Recognition (CVPR)*, pages 11164–11173, 2022. 2
- [62] Sangdoon Yun, Dongyoon Han, Seong Joon Oh, Sanghyuk Chun, Junsuk Choe, and Youngjoon Yoo. Cutmix: Regularization strategy to train strong classifiers with localizable features, 2019. 2, 3, 4, 7
- [63] Bowen Zhang, Yidong Wang, Wenxin Hou, HAO WU, Jindong Wang, Manabu Okumura, and Takahiro Shinozaki. Flexmatch: Boosting semi-supervised learning with curriculum pseudo labeling. In *Advances in Neural Information Processing Systems*, pages 18408–18419. Curran Associates, Inc., 2021. 2
- [64] Cong Zhang, Hongsheng Li, Xiaogang Wang, and Xiaokang Yang. Cross-scene crowd counting via deep convolutional neural networks. In *Proceedings of the IEEE Conference on Computer Vision and Pattern Recognition (CVPR)*, 2015. 1
- [65] Hongyi Zhang, Moustapha Cisse, Yann N. Dauphin, and David Lopez-Paz. mixup: Beyond empirical risk minimization. In *International Conference on Learning Representations*, 2018. 2, 3, 4, 7
- [66] Shimao Zhang, Changjiang Gao, Wenhao Zhu, Jiajun Chen, Xin Huang, Xue Han, Junlan Feng, Chao Deng, and Shujian Huang. Getting more from less: Large language models are good spontaneous multilingual learners. In *Proceedings of the 2024 Conference on Empirical Methods in Natural Language Processing*, pages 8037–8051, Miami, Florida, USA, 2024. Association for Computational Linguistics. 3
- [67] Shiwei Zhang, Wei Ke, Shuai Liu, Xiaopeng Hong, and Tong Zhang. Boosting semi-supervised crowd counting with scale-based active learning. In *Proceedings of the 32nd ACM International Conference on Multimedia*, pages 8681–8690, New York, NY, USA, 2024. Association for Computing Machinery. 1, 2, 7
- [68] Yingying Zhang, Desen Zhou, Siqin Chen, Shenghua Gao, and Yi Ma. Single-image crowd counting via multi-column convolutional neural network. In *Proceedings of the IEEE Conference on Computer Vision and Pattern Recognition (CVPR)*, 2016. 2, 6
- [69] Huilin Zhu, Jingling Yuan, Zhengwei Yang, Xian Zhong, and Zheng Wang. Fine-grained fragment diffusion for cross domain crowd counting. In *Proceedings of the 30th ACM International Conference on Multimedia*, page 5659–5668, New York, NY, USA, 2022. Association for Computing Machinery. 8
- [70] Huilin Zhu, Jingling Yuan, Xian Zhong, Zhengwei Yang, Zheng Wang, and Shengfeng He. Daot: Domain-agnostically aligned optimal transport for domain-adaptive crowd counting. In *Proceedings of the 31st ACM International Conference on Multimedia*, page 4319–4329, New York, NY, USA, 2023. Association for Computing Machinery. 8
- [71] Huilin Zhu, Jingling Yuan, Xian Zhong, Liang Liao, and Zheng Wang. Find gold in sand: Fine-grained similarity mining for domain-adaptive crowd counting. *IEEE Transactions on Multimedia*, 26:3842–3855, 2024. 8

- [72] Pengfei Zhu, Jingqing Li, Bing Cao, and Qinghua Hu. Multi-task credible pseudo-label learning for semi-supervised crowd counting. *IEEE Transactions on Neural Networks and Learning Systems*, 35(8):10394–10406, 2024. [2](#), [7](#)